

**Małgorzata Szczepańska<sup>1</sup>, Mirosław Rurek<sup>1,a</sup>**

<sup>1</sup> Faculty of Geographical Sciences, Kazimierz Wielki University in Bydgoszcz, Poland.

ORCID: <sup>a</sup> <https://orcid.org/0000-0002-7092-4853>

Corresponding author: Małgorzata Szczepańska, e-mail: [gosiaszcz42@wp.pl](mailto:gosiaszcz42@wp.pl)

---

## Using Sentinel-2 satellite imagery in the analysis of forest cover changes following the storm of 2017 – case study of the Przymuszowo Forest Inspectorate in Poland

---

**Abstract:** Climate change is causing increasingly frequent extreme events (including strong winds), which are becoming an integral part of the natural environment. In 2017, from the 11<sup>th</sup> to 12<sup>th</sup> of August, a storm passed causing catastrophic damage in general and to forest resources in particular. The study aims to determine the feasibility of using Sentinel-2 satellite imagery and other GIS tools and techniques for estimating forest damage caused by the storm in the Przymuszowo Forest Inspectorate. The analysis of forest cover changes was performed using the NDVI and BI2 index as well as unsupervised classification predicated on satellite imagery obtained before and after the storm. It was calculated that a total of 2,048.1 hectares of forest was damaged based on the NDVI index and 1,661.7 hectares based on the unattended classification, whereas the area of agricultural land and non-forest land based on the BI2 index was 1,739.1 hectares. These figures are comparable to the records of post-storm losses from the Przymuszowo Forest Inspectorate. This indicates a considerable feasibility of Sentinel-2 satellite imagery in assessing damage caused by extreme phenomena (strong winds) in forest areas, which is true both on a regional and global scale owing to the wide range of imaging (up to 290 km). The only limitation for Sentinel-2 satellites is heavy cloud cover, as the emitted radiation does not penetrate clouds.

**Keywords:** storm, Sentinel-2, NDVI, BI2, unsupervised classification

### 1. Introduction

Climate change and warming cause increasingly frequent extreme phenomena, which are becoming an integral part of the natural environment. Said changes entail both regional and global threats, making weather considerably unpredictable (Diemientiew, 2018). Extreme phenomena constitute relatively rare, short-term events and occur with high random variability (Kundzewicz and Matczak, 2010). The available literature highlights the increasing frequency of extreme events, which include heavy rains, droughts, land degradation processes, floods, mass movements, soil erosion and high winds (Clarke and Rendell, 2007). The later mentioned strong winds are particularly frequent in Europe, and numerous scientific studies show that with the climate warming, the number of these extreme events in Europe is

likely to increase (Clarke and Rendell, 2007; Haarsma et al., 2013; Forzieri et al., 2017).

The storm of August 11–12, 2017 was one of the most destructive natural phenomena in recent decades. As a result of the storm, 6 people were killed, residential and farm buildings, local and community roads, agricultural crops, power lines and poles, public utility complexes and many others were destroyed. The relatively largest losses were recorded in forest resources (Trębski, 2017).

Remote sensing methods have played an important role in studies pertaining to changes in land use forms, allowing for the analysis of land cover changes (including forest cover). Remote sensing methods are also more widely used, as evidenced by the increase in studies incorporating satellite data (Šimić-Milas et al., 2015, Zhang et al., 2021). This is due to the

launch of new satellite systems (e.g., Sentinel-1, Sentinel-2, Landsat-8) and better availability of open-source applications that allow for the analysis of such data (QGIS, SAGA GIS) (Czapiewski and Szumińska, 2022). The most frequently explored aspect of vegetation cover studies using modern remote sensing methods involves determining the extent of occurrence of particular vegetation types, changes in extent, as well as the causes and effects of these changes (Tomaszewska et al., 2011). In the case of forests, detecting, identifying and quantifying forest damage from a remote sensing platform offers an opportunity to monitor and assess forest damage on a global scale (Roy et al., 2014).

Methods of obtaining satellite data involve the use of electromagnetic radiation, which is reflected from the earth's surface and thus recorded by a sensor aboard the satellite (Hejmanowska and Wężyk, 2020). The source of electromagnetic radiation is the Sun, which emits energy in different ranges of electromagnetic wavelengths. Remote sensing uses wavelength ranges that freely penetrate the atmo-

sphere (the so-called atmospheric windows). The ranges in question include visible light, near infrared and mid-infrared (Ciołkosz, 2005; Zarzecki and Pasierbski, 2009; Hejmanowska and Wężyk, 2020). One of the most popular satellite missions is Sentinel-2, which consists of twin satellites placed in the same orbit: Sentinel-2A (in 2015) and Sentinel-2B (in 2017), both recording radiation in the optical range. The advantages of the Sentinel-2 mission include short revisit time (each fragment of the earth is recorded every 5 days), wide imaging bandwidth (up to 290 km) and high spatial resolution (10 m in the visible range and 20 m in the infrared and near-infrared). The disadvantage of satellite imagery is the possible occurrence of cloud cover, depending on current meteorological situation at the time the images are taken (Hejmanowska and Wężyk, 2020).

The purpose of the study is to determine the feasibility of using Sentinel-2 imagery to assess the extent and impact of forest damage caused by the 2017 storm, using GIS tools and techniques.

## 2. Study scope and methods

### 2.1. Study scope

The spatial scope of the work includes the area of the Przymuszewo Forest Inspectorate, located on the territory of the Regional Directorate of State Forests (RDSF) in Toruń. Administratively, the study area is located within the boundaries of Pomerania Voivodeship, in two communes: Brusy and Chojnice (Fig. 1). The soil shows the prevalence of sand and gravel sediments, which form the Brda outwash plain (Galon, 1953, Karasiewicz et al., 2015). This geological structure favours the formation of

relatively poor and podzolic soils (Galon, 1953; Dysarz, 1998, Jankowski et al., 2015). These soils are currently covered mainly by artificially introduced coniferous monocultures.

The main forest-forming species (95.18%) in the study area is the Scots pine (*Pinus sylvestris* L.), accounting for as much as 97.3% of the forest area, with the second most common species being the warty birch (*Betula pendula* Roth) with a share of 1.2%. Other species account for only 1.5%. (Regionalna..., 2019).

### 2.1. Study methods

#### 2.1.1. Source materials

The primary material used for the study was Sentinel-2 satellite imagery, provided free of charge by the Copernicus Open Access Centre (ESA, <https://scihub.copernicus.eu/dhus/#/home>), which was processed using QGIS 2.8

and SAGA 7.6.3 software. Based on these, the authors calculated the NDVI and BI2 indices, and carried out unsupervised classification. The imagery was acquired for the period between May 2017 and March 2019. All of the

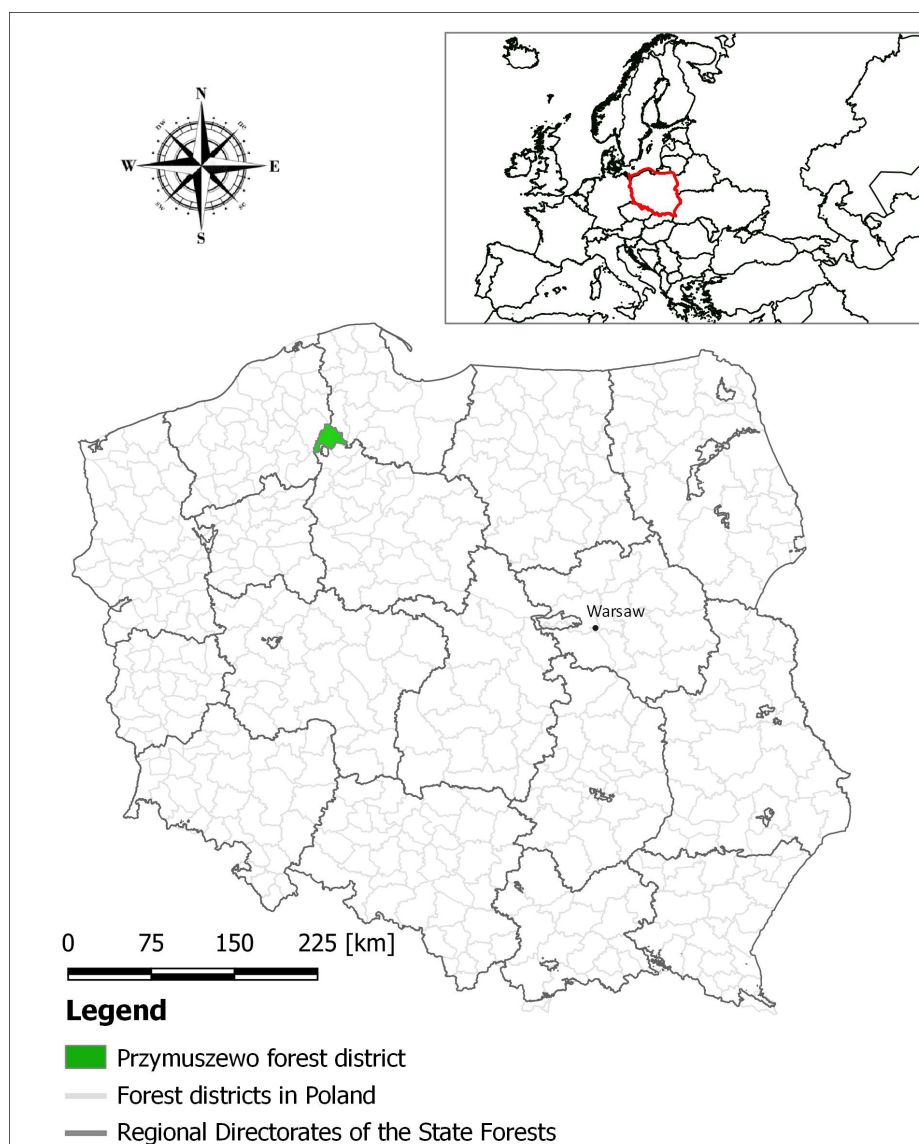


Fig. 1. Location of the study area in Poland

Sentinel-2A/B images used were obtained at the MSIL2A level (taking into account atmospheric correction). Apart from the extent of cloud cover, the selection of imagery was also determined by the date of image registration. This is due to the fact that multi-temporal analyses ought to be predicated on images from the same vegetation season. For further analysis, we selected imagery recorded as close as possible to the date before the hurricane, in the spring and summer seasons: 01.05.2017 and 30.07.2017 (the satellite image from July shows a slight cloud cover in the southern part of the area), and images from 28.09.2017, 17.03.2018, 05.07.2018 and 02.03.2019, corresponding to the situation after the passage of the storm. The analysis included a total of 6 satellite images from the Sentinel-2 satellite recorded

before and after the passage of the hurricane. Preliminary assessment of images from other dates (21.04.2018, 04.08.2018, 13.10.2018, 30.06.2019, 24.08.2019) resulted in their exclusion from the analyses due to the presence of cloud cover.

Furthermore, the authors obtained and analysed meteorological data from the Institute of Meteorology and Water Management (<https://danepubliczne.imgw.pl/>), photos of the passage of the atmospheric front (<https://www.wetterzentrale.de/>) and data provided by the State Forestry – Przymuszewo Forest Inspectorate. The data from the forest inspectorate concerned losses in forest resources, which were found on the basis of direct calculations made after the passage of the storm.

### 2.1.2. Characteristics of the indicators used for satellite data analysis

The first of the indices used in the study was the Normalized Difference Vegetation Index (NDVI). The index is calculated based on the spectral ranges of red (RED) and near-infrared (NIR). The index assumes values from -1 to 1, where the higher the value of the index, the greater the amount of biomass (values closer to +1 indicate the density of green vegetation) (Rouse et al., 1974; Pettorelli et al., 2011, Tomaszewska et al., 2011). NDVI is commonly used in environmental analyses and is a standard tool in remote sensing monitoring of vegetation condition assessment. The index has been recognized as the optimal spectral index used for monitoring forest damage and deforestation (Ciesielski et al., 2016; Xue and Su, 2017; Olmo et al., 2021). The NDVI index is derived from the following formula:

$$NDVI = \frac{(NIR - VIS)}{(NIR + VIS)}$$

where:

VIS – channel value in the red band (band B4 in Sentinel-2)

NIR – channel value in the infrared band (band B8 in Sentinel-2)

The adopted method consists in indicating the differences in the index values and reclassifying the data for forest areas on the basis of satellite images before and after the storm. The selection of values used in the reclassification was based on 7 longitudinal profiles located throughout the analysed forest district. Each profile was sampled every 10 m by a circle with a radius of 5 m, and the minimum, maximum, mean and median values in each circle were obtained for the statistics. The minimum value of the NDVI index for forested areas was 0.513, while the maximum value was 0.666. The analysis involved pre-storm images overlaid with a mask of actual forest cover to demonstrate the changes.

Another indicator used in the study was the BI2 brightness index. It represents the average brightness of a satellite image, highlighting the class of land stripped of vegetation. For analyses, the algorithm selects natural surface areas to distinguish between agricultural and non-forest land (Escadafal, 1989; Xie et al., 2022). This indicator is particularly sensitive to

the brightness of soils, which is synchronized with the presence of salt on the land surface and moisture content. The BI2 index is derived from the following equation:

$$BI2 = \sqrt{\frac{(VIS^2 + GRN^2 + NIR^2)}{3}}$$

where:

VIS – channel value in the red band (band B4 in Sentinel-2)

NIR – channel value in the infrared band (band B8 in Sentinel-2)

GRN – channel value in the green band (band B3 in Sentinel-2)

As in the case of NDVI, the method adopted was to indicate differences in the value of the indicator and subsequently reclassify the data for non-forest areas (all other area except forest) based on satellite images before and after the storm. The selection of values for reclassification was predicated on 7 longitudinal profiles located in non-forest areas located throughout the studied forest district, sampled in the same way as described above. The minimum value of the BI2 index for non-forest areas was 0.106, while the maximum value was 0.600. The two aforementioned indices were used to identify the extent of forested (NDVI) and non-forest areas (BI2) in the periods before and after the storm.

The final stage in the analysis of changes in the use of the study area surface was unsupervised classification. The technique in question serves as a basis for developing a model of classes that display similar spectral structure (similarity of image features). Each class refers to a cluster parameter, i.e., a specific interpretation of a given object (Kaufman and Rousseeuw, 1990; Likas et al., 2003, Urbański, 2011; Frąckiewicz and Palus, 2011). The employed method consisted in creating a land cover map with the appropriate value assigned to a pixel in the satellite imagery. On satellite images in all Sentinel-2 spectral channels (bands 1 to 12), a terrain profile was established using the “Profile tool” plug-in that allows interaction of the profile (spectral reflectance values) with the line on the satellite imagery. It was observed that four spectral channels: 4, 5, 11 and 12 demon-

strate increasing values given the change in land use from a forest area to a non-forest area, and therefore the above four spectral channels were selected for the analysis of unsupervised classification. Classes (pixels) corresponding to each vegetation type were combined into clus-

ters. The result of the analysis was raster data divided into 10 classes, with 3 of the 10 classes representing forest areas. For the purpose of the study, a reclassification of the data into classes was performed by concatenating the pixels representing the forest class.

### 3. Characteristics of the storm in August 2017

#### 3.1. Meteorological situation

August 2017 was an extreme month in terms of meteorological phenomena as compared with previous years. It was characterized by high values of precipitation and the highest wind speed (Szczepeńska, 2022a). In 2017, the gauging station closest to the analysed area recorded as much as 819 mm of total precipitation (August: 112.9 mm), while the annual average for the multi-year period (2010–2021) was 601 mm. The recorded maximum wind speed reached 29 m/s (IMGW, 2020; Szczepeńska, 2022b). However, this was likely not the highest wind speed in the areas affected by

the storm, as verbal account from the Director of the Regional Directorate of State Forests in Toruń indicates a much higher speed, exceeding 83 m/s.

The month was very warm. Beginning on August 9th, Poland came under the influence of lows from the North Sea and then from south-eastern Europe. In the following days (August 10–11), hot tropical air began to flow in from the southeast, while a polar-maritime atmospheric front preceded by a line of squalls was approaching from the west (Fig. 2A; IMGW, 2020). The cool storm system accompanied

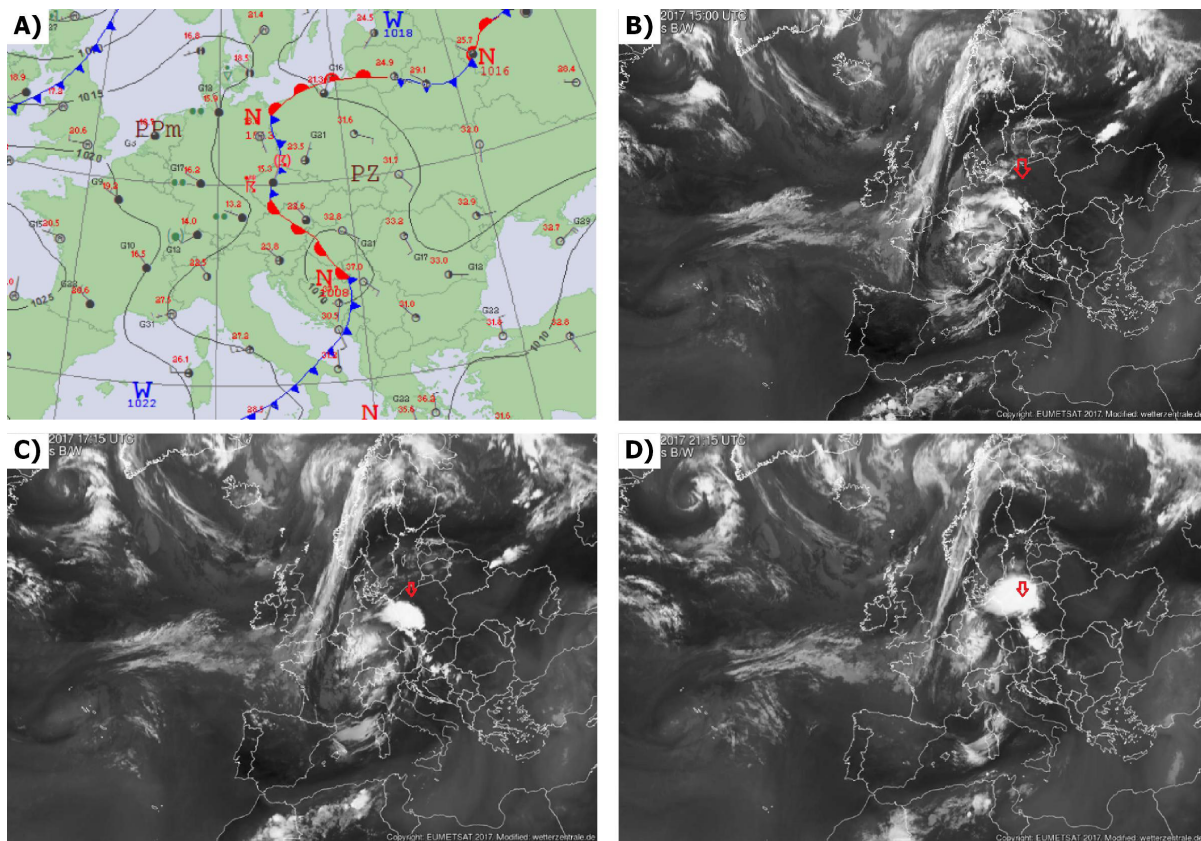


**Fig. 2.** A – synoptic map at 12:00 UTC on August 11th, 2017. (IMGW, 2020); B – passage of the front from the EUMETSAT satellite at 15:00 UTC on August 11th, 2017; C – passage of the front from the EUMETSAT satellite at 17:15 UTC on August 11th, 2017; D – passage of the front from the EUMETSAT satellite at 21:15 UTC on August 11th, 2017 (wetterzentrale.de, 2020).

by the undulating atmospheric front began to displace the hot tropical air. The confluence of the two air masses resulted in a dangerous weather phenomenon, bringing high precipitation totals and very strong winds, which were characterized by short-term variability and high gustiness (IMGW, 2017; Chojnacka-Ożga and Ożga, 2018; Sulik and Kejna, 2020).

On the day of the phenomenon's passage (i.e., August 11–12), the storm system began

to form as early as the afternoon, with its onset on the borders of eastern Germany, north-western Czech Republic and southeastern Poland. The system headed from the southwest toward the northeastern and eastern parts of Poland, passing through the voivodeships of Lower Silesia, Opole, Greater Poland, Kuyavia-Pomerania and Pomerania, thus reaching the area of the Przymuszewo Forest Inspectorate (Fig. 2B, 2C, 2D).

**Table 1.** Measured wind speeds and precipitation at the meteorological station in Chojnice from 18:00 on August 11th, 2017 to 06:00 on August 12th, 2017 (IMGW, danepubliczne.imgw.pl, 2020)

Time UTC	Temperature [°C]	Mean wind speed [m/s]	Gust wind speed [m/s]	Wind direction	Rainfall 1 hour [mm]
18:00	23.6	1.5	2.6	NNW	0.0
19:00	22.0	3.4	2.6	NNW	0.0
20:00	21.9	4.1	5.9	NNW	0.0
<b>21:00</b>	<b>16.5</b>	<b>12.5</b>	<b>24.3</b>	<b>WSW</b>	<b>19.9</b>
22:00	16.9	4.6	7.0	NNW	-
23:00	16.6	4.8	7.3	N	0.4
00:00	16.9	3.0	4.3	NNW	0.0
01:00	16.4	3.8	7.0	SSW	0.0
02:00	16.6	4.0	5.9	SSW	0.0
03:00	16.5	3.0	5.0	ENE	0.3
04:00	16.9	2.4	3.6	SSW	0.0
05:00	17.1	3.5	5.5	WSW	0.0
06:00	17.1	2.9	4.3	WSW	0.0

During the passage of the storm, at the measuring station in Chojnice, the air temperature did not fall below 16.0°C, and the wind speed increased rapidly. As can be observed from the data in Table 1, the highest values of individual meteorological elements were recorded between 21:00 and 22:00. The air temperature at

21:00 was as high as 16.5°C. The wind speed at its peak reached 24.30 m/s, while rainfall sums at the time amounted to 19.9 mm per hour. As this was a violent and short-lived phenomenon, the situation began to stabilize just half an hour after the storm occurred.

### 3.2. Characteristics of forest stand damage based on data from Przymuszewo Forest Inspectorate

The total area of the Przymuszewo Forest Inspectorate is 18,600 hectares, with forested areas covering 17,700 hectares. Information obtained from the Forest Inspectorate indicates that 1,231.37 hectares of forest area were destroyed. This area was determined in the course of direct calculations in individual forest districts over two years. This represents approx. 7% of the pre-storm forest area. The Przymuszewo Forest Inspectorate was ranked 5th in

terms of damage in [ha] caused on the territory of the Regional Directorate of State Forests in Toruń, following the forest districts of: Rytel, Czersk, Runowo and Szubin (Kaczmarek, 2018). The most extensive damage in the studied forest inspectorate was recorded in its northern and central parts (Łabaj, 2017). The damage was in the form of windrows and windbreaks, as well as severe deformation of tree trunks, often accompanied by the tearing of the

root system (saltation uproots) and breaches in stability (Wesołowski and Żmihorski, 2018;

Trębski, 2019). Entire forest communities were destroyed, not just individual trees (Fig. 3A).

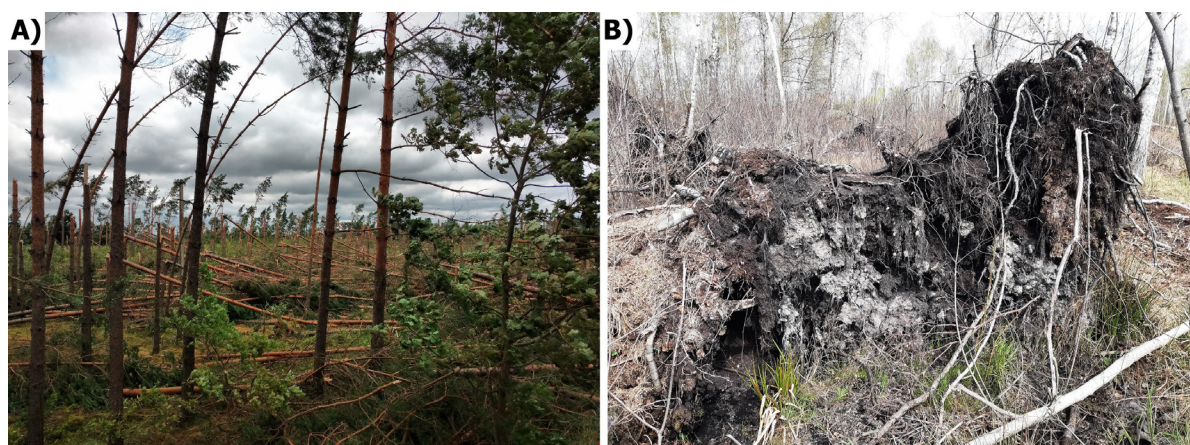


**Fig. 3.** Destruction of forest resources after the storm: A – destroyed forest (Brusy Municipality, 2018), B – overturned tree with its root system (M. Szczepańska, 2020)

Damage was caused to stands in all age classes, while the degree of susceptibility to the type of damage varied depending on the class of trees. In the case of stands in the lower age classes (Class I and II, aged 1–20 and 21–40 years, respectively), “blasting,” that is, severe tilting of trees with deformation of trunks and crowns, was recorded. This type of damage occurs when trees remain in the vitality stage, yet do not guarantee cultivation potential (Łabaj, 2017). In stands of higher classes (Class

III, age 41–60), damage in the form of breaking, deformation and complete toppling along with the root system was recorded (Fig. 3B).

The data presented in Table 2 shows that the greatest damage was sustained by the Scots pine stand. Its damage was estimated at 570,225 m<sup>3</sup>, of which the total amount of damage was estimated at 589,012 m<sup>3</sup>. Smaller losses were suffered by other species (due to their aggregately smaller share in the stand).

**Table. 2.** Summary of damage to tree species in Przymuszewo Forest Inspectorate (data from Przymuszewo Forest Inspectorate)

Species	Small sized wood [m <sup>3</sup> ]	Midium sized wood [m <sup>3</sup> ]	Large sized wood [m <sup>3</sup> ]	Total damage [m <sup>3</sup> ]
Beech ( <i>Fagus L.</i> )	74	89	326	489
Birch ( <i>Betula L.</i> )	1,843	1,564	6,662	10,069
Oak ( <i>Quercus L.</i> )	13	85	96	194
Red oak ( <i>Quercus rubra L.</i> )	1	5	7	14
Hornbeam ( <i>Carpinus betulus L.</i> )	0	0	2	3
Lime tree ( <i>Tilia cordata Mill.</i> )	2	0	13	15
Larch ( <i>Larix Mill.</i> )	53	383	526	962
Alder ( <i>Alnus Mill.</i> )	164	623	1,409	2,196
Scots Pine ( <i>Pinus sylvestris L.</i> )	26,370	297,441	246,414	570,225
Weymouth Pine ( <i>Pinus strobus L.</i> )	7	455	122	583
Spruce ( <i>Picea abies L.</i> )	279	1,938	2,046	4,264
<b>All</b>	<b>28,805</b>	<b>302,584</b>	<b>257,623</b>	<b>589,012</b>

Summarizing the scale of destruction in the Przymuszewo Forest Inspectorate, it was estimated that the number of trees that were

knocked down over one night, under normal conditions, would have been harvested over a period of 10 years (Starostwo..., 2018).

## 4. Results of satellite imagery analysis

The calculated values for NDVI, BI2 and unsupervised classification are presented in Table 3.

**Table 3.** Area of forests and non-forest areas in Przymuszewo Forest Inspectorate calculated on the basis of Sentinel-2 images

Date	Forest area based on the NDVI index [ha]	Area of agricultural land and non-forest areas based on the BI2 index [ha]	Forest area based on unsupervised classification [ha]
2017_05_01	<b>13,581.3*</b>	<b>13,848.2*</b>	<b>19,311.6*</b>
2017_07_30	14,980.3	15,766.7	17,544.3
2017_09_28	16,013.8	13,645.5	18,323.9
2018_03_17	14,761.5	11,784.2	18,423.7
2018_07_05	<b>11,533.2*</b>	18,373.2	17,884.9
2019_03_02	12,689.5	<b>15,587.3*</b>	<b>17,649.9*</b>
The difference in area	2,048.1 (15.1%)	1,739.1 (12.6%)	1,661.7 (8.6%)
The area of loss determined by the Nadleśnictwo Przymuszewo District		1,231.27 (6.9%)	

\* – the results of indicators that were used to calculate surface area differences.

Based on the calculated NDVI, the area covered by forest in the Przymuszewo Forest Inspectorate decreased by 2,048.1 hectares, which is 15.1% of the forest before the 2017 storm (Table

3 and Fig. 4). For the period before the storm, Sentinel-2 images were considered for the dates of 01.05.2017 and 30.07.2017. A larger calculated forest area was obtained for July, and a smaller

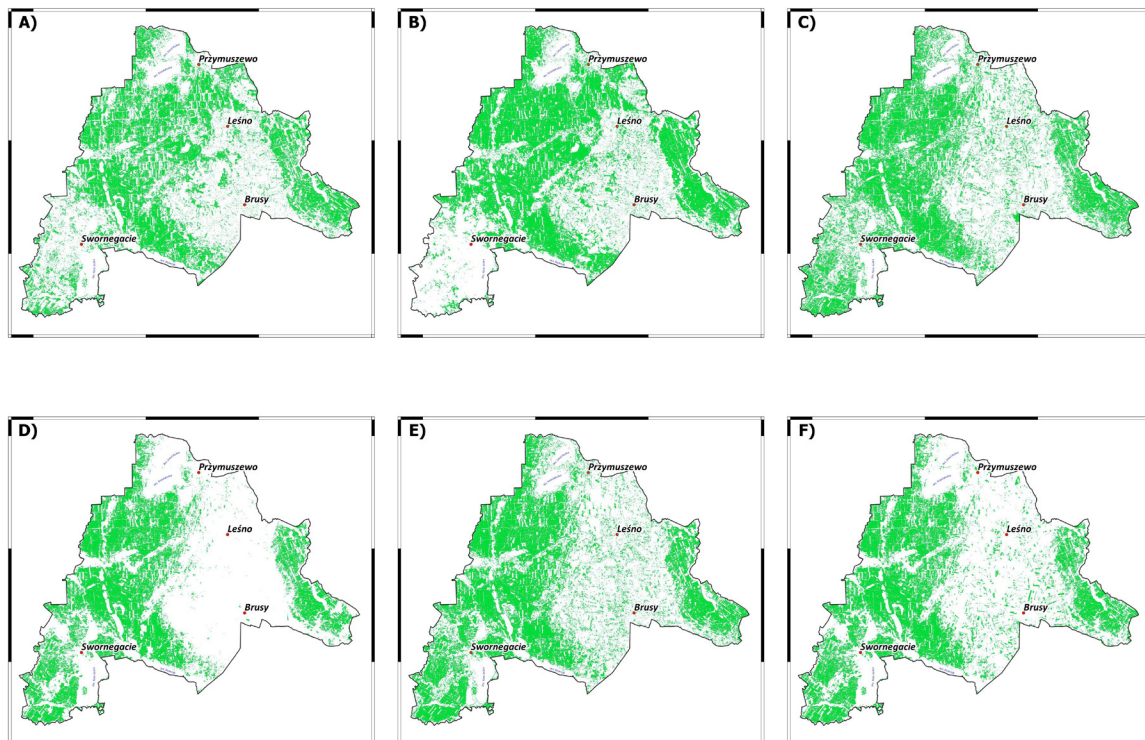


**Fig. 4.** Changes in the extent of forest areas determined on the basis of the NDVI index in the area of the Przymuszewo Forest Inspectorate on the basis of Sentinel-2 images taken on the dates: A – 01.05.2017, B – 30.07.2017, C – 28.09.2017, D – 17.03.2018, E – 05.07.2018, F – 02.03.2019, green – forest areas, white – other areas.



one for May, which may be related to both the high level of vegetation development in July and the presence of cloud cover on the second of the satellite imaging dates (in the southwestern part of the area). On the first survey date after the storm, i.e., 28.09.2017, there was still a significant proportion of forested areas in the area classified on the basis of the NDVI index. This is due to the presence of trees that had not yet been cleaned up and, consequently, the high value of the vegetation index. On the next two dates (i.e., 17.03.2018 and 05.07.2018), a reduction in the extent of forested areas is evident, which is indicative of the cleanup work carried out in the forests. Taking into account the above observations pertaining to the suitability of the images from different dates, the authors elected to employ the NDVI index calculated for the images from 01.05.2017 and 05.07.2018 (values shown in bold in Table 3). However, the values calculated for the 02.03.2019 image were dismissed, as the summed value of afforestation on this date was due to both storm damage as well as reforestation and natural succession of low vegetation.

As the calculated BI2 shows, the area of agricultural and non-forest land increased from 13,848.2 hectares to 15,587.3 hectares, or 12.6%,

between 01.05.2017 and 02.03.2019. (Table 3, Fig. 5). As in the case of the NDVI index, differences were indicated between the actual state of land use and the use determined from satellite imagery. This was due to factors such as cloud cover, the period when the photo was taken, the progress of work associated with cleaning up the forests after the storm, as well as summer harvest-related works and haying, and the vegetation level of the cultivated crops. The first date – 01.05.2017 – was selected for the analysis of calculations pertaining to forest cover differences (Fig. 5A), and the initial area of non-forest land was estimated at 13,848.2 hectares. In subsequent imaging performed in July, both 2017 (30.07.2017) and 2018 (05.07.2018) show an increase in the extent of areas characterised with high BI2 values. High values of this indicator suggests drying of soils (related to both weather conditions and exposed land surface – forest destruction). The difference in the value of the index between 2017 and 2018 may be related to the marked difference in total precipitation in the two years. The year 2018 was also warmer than 2017, resulting in higher evaporation values (Okoniewska and Szumińska, 2020). The increase in BI2 value may also be the

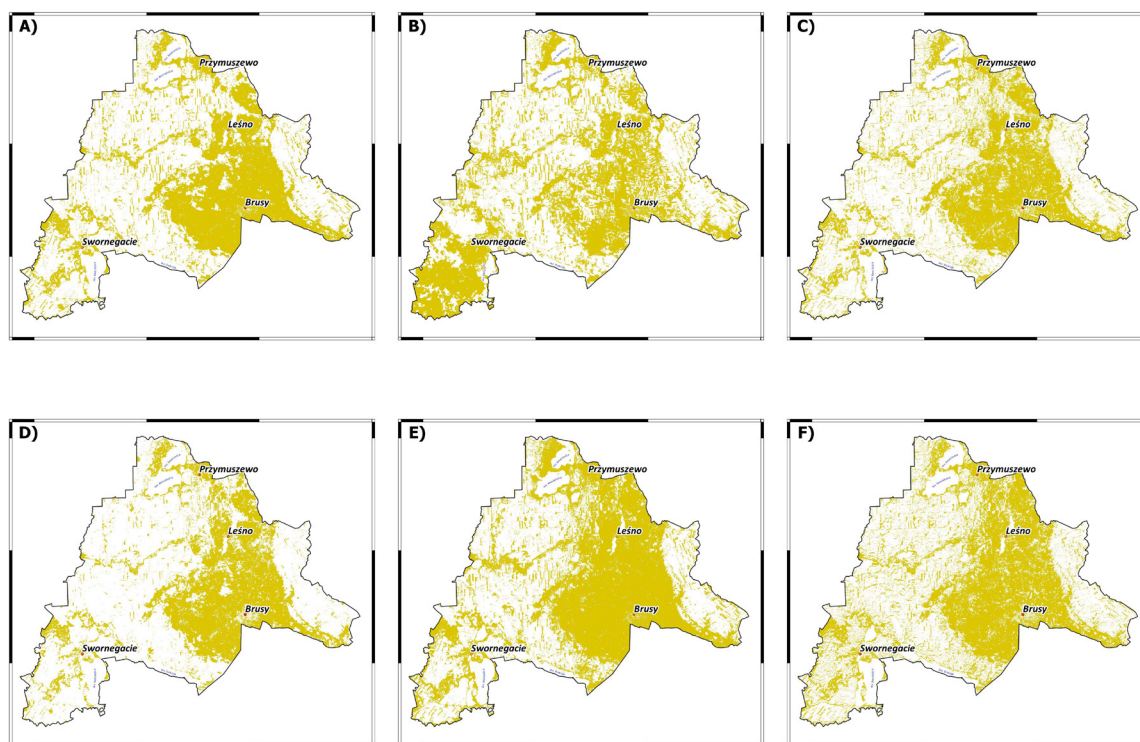


**Fig. 5.** Changes in the extent of non-forest areas determined on the basis of BI2 in the area of Przymuszewo Forest Inspectorate on the basis of Sentinel-2 images taken on the dates: A – 01.05.2017, B – 30.07.2017, C – 28.09.2017, D – 17.03.2018, E – 05.07.2018, F – 02.03.2019, yellow – non-forest areas, white – other areas.

effect of meadow mowing during the summer (which is conducive to drying of the surface soil layer). Due to the limitations regarding the use of the BI2 index described above, for the calculation of the difference in the surface of non-forest areas before the and after the storm, it was assumed that the non-forest surface area increased by 1,739.1 hectares (Table 3, Fig. 5).

From the data collected using unsupervised classification, it is clear that the area of forest land, similarly to that calculated from NDVI, decreased, but the calculated values of forest surface area are slightly higher compared to the results obtained from NDVI (Table 3, Fig. 6). This is due to the nature of the method, which uses not only a narrow range of indicator values, but the spectral range of the

entire channel. The surface of forest areas as of 01.05.2017 was 19,311.6 hectares. On the next date – 30.07.2017, the area decreased, but such a result was due to the cloud cover present in the image in the southwestern part of the area on this day. On the next dates (28.09.2017 and 17.03.2018), the results show a reduction in the forested surface area, with even smaller forest coverage obtained on the subsequent dates – 05.07.2018 and 02.03.2019. This indicates that the post-storm areas have been cleaned up, but the total forest coverage is also likely to be due to new plantings and self-foresteing. The difference in forest surface area based on the images from the first and last dates (i.e., 01.05.2017 and 02.03.2019) amounted to 1,661.7 hectares, or 8.6% (Table 3).

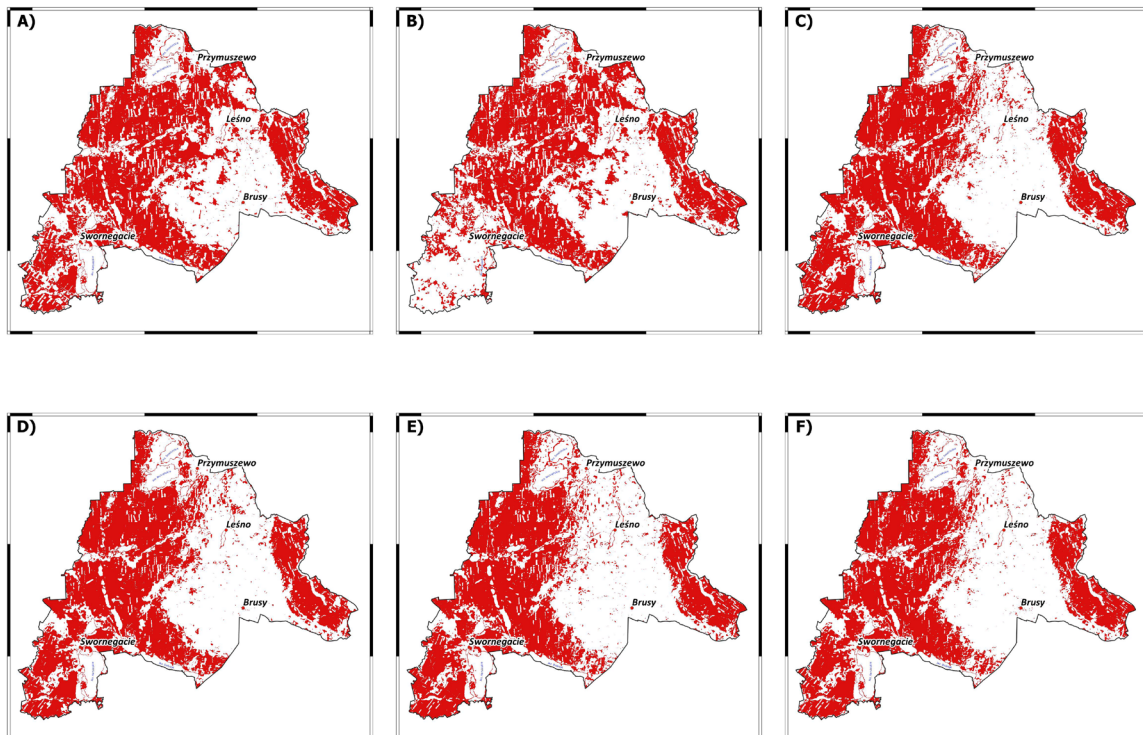


**Fig. 6.** Changes in the extent of forest areas determined on the basis of unsupervised classification in the Przymuszewo Forest Inspectorate on the basis of Sentinel-2 images taken on the dates: A – 01.05.2017, B – 30.07.2017, C – 28.09.2017, D – 17.03.2018, E – 05.07.2018, F – 02.03.2019, red – forest areas, white – other areas.

## 5. Discussion

Based on the NDVI index derived from Sentinel-2 satellite imagery, it was calculated that forest areas of 2,048.1 ha (15.1%) were damaged. Unsupervised classification, on the other hand, the value was estimated at 1,661.7

ha (8.6%). According to the data of the RDSF in Toruń (Kaczmarek, 2018), forest areas in the Przymuszewo Forest Inspectorate were reduced by 1,760 ha. With the above in mind, the results of the unsupervised classification are

more similar to the losses estimated by the State Forests. Furthermore, based on the BI2 index, it was found that the area of non-forest land increased by 1,739.1 (12,6%) hectares. This is higher than the value determined by the Przymuszewo Forest Inspectorate, i.e., 1,231.27 ha (6.9%). The differences in the results obtained from the satellite images are related to the conditions at the time of imaging, such as cloud cover, the state of vegetation, the stage of clean-up after storm and reforestation of post-storm areas. It should be noted, however, that the differences in forest and non-forest areas calculated within the framework of this study, based on the unsupervised classification and the BI2 index, respectively, are more consistent with each other than the forest inspectorate data, that is, they demonstrate a similar loss of forest area and gain of non-forest area after the storm.

Remote sensing methods, taking into account satellite images before and after the passage of the storm, have been used for analyses of forest area changes by various authors (Hościło and Lewandowska, 2018; Dalponte et al., 2020; Giannetti et al., 2021; Piragnolo et al., 2021; Olmo et al., 2021). The study by Hościło and Lewandowska (2018) showed that the area of damage in the Przymuszewo Forest Inspectorate calculated using the NDMI spectral index (source material – Sentinel-2 imagery) amounted to 3,268.0 hectares, of which 2,100.0 hectares within the National Forests and 1,168.0 hectares outside the National Forests. The results of the analyses conducted by the cited authors show that the amount of damage in the State Forests is severely underestimated, while in the non-State Forests it is overestimated. However, the extent of forest damage determined on the basis of the NDMI for the Przymuszewo Forest Inspectorate is higher than the results obtained within the framework of the present study, based on the NDVI indicators and unsupervised classification. This is likely due to the nature of the indices used, with NDMI being used more often to study leaf water content and changes in the spongy structure of mesophyll, and NDVI for changes in vegetation condition (resulting from the amount of chlorophyll). Hościło and Lewandowska (2018) also note that the estimated extent of damage included indicative

data determined in the first days after the storm (i.e., 24.08.2017 and 28.09.2017). Dalponte et al. (2020) show that more accurate results of damage caused by the storm can be obtained 8 months after the event by comparing two images taken during the summer, including one image before and one after the event (accuracy exceeding 80%), while less accurate results can be obtained using images taken closer to the extreme event (within the first two weeks after the storm). Similar conclusions were reached by Giannetti et al. (2021) as they found that the most accurate results for analysing forest cover changes after a windstorm from satellite imagery can be obtained 7 months after the event at the earliest. In contrast, Olmo et al. (2021) used a two-period approach between vegetation indices. Their results show that based on a multi-period analysis predicated on vegetation indices, a deviation in reflectance values can be observed for damaged and undamaged areas compared to years before the storm.

Sentinel-2 satellite imagery presents new perspectives in forest monitoring (Wang et al., 2010; Hościło and Lewandowska, 2018; Dalponte et al., 2020; Giannetti et al., 2021; Piragnolo et al., 2021; Olmo et al., 2021). The ideal situation involves analysing images taken at exactly the same time and under the same conditions for each of the periods studied. Unfortunately, when collecting the data, it is necessary to take into account the optimal timing of the images taken, as well as cloud cover (which makes it impossible to obtain reliable results), unfavourable meteorological conditions (e.g., a later beginning of vegetation season), and extent of clean-up work performed in the forests. It should be noted that the most visible effects of the passage of the hurricane are destroyed tree crowns, damaged trunks and a reduction in the assimilation apparatus of trees (Wesołowski and Żmihorski, 2018). As a result of this damage, the contribution of the assimilatory apparatus to the values of spectral reflectance from the stands decreases. In forests where nearly the entirety of the tree stand was destroyed the lower forest floor becomes exposed (having suffered less damage), which contributes to an increase in spectral reflectance from the ground cover. Hence, the results obtained may differ slightly from the data compiled by foresters.

## 6. Conclusions

Based on the results, it was concluded that Sentinel-2 data allow for accurate distinction between forested areas and agricultural land and non-forest land. In the case of the studied indicators, the unsupervised classification proved to yield results more similar to the estimates of stand losses made by the State Forests, compared to the results obtained from the NDVI indicator. The BI2 index, on the other hand, was found to be useful in determining changes within non-forest areas. Differences in the results between NDVI, BI2 and the unsupervised classification were due to the characteristics of the methods used. The NDVI index for calculations uses reflection values in the red (band 4) and near-infrared (band 8) ranges, which encompass bands offering much information on the condition of the vegetation. The BI2 indicator uses values in the red range (band 4), infrared range (band 8) and green range (band 3), highlighting the brightness of soils, which is synchronized with the presence of salt on the ground surface. On the other hand, as many as four spectral channels (bands 4, 5, 11 and 12) were used to calculate the unsupervised classification, as they indicated increasing values at the site of transition from the forested to non-forest area. This highlights the need to use not one, but a set of indicators,

which may offer results that are closest to the actual state.

The results of the analyses confirmed that the use of remote sensing methods and the calculation of spectral indices based on Sentinel-2 satellite imagery is a useful tool in determining the area of forest damage caused by hurricane winds. The methods employed can be used in the future to relatively quickly determine losses during similar extreme events causing tree stand damage, as well as to further monitor the state of vegetation on restored forest areas.

The wide imaging bandwidth of Sentinel-2 satellites (reaching 290 km), high frequency of image acquisition of the same fragment of the Earth's surface (every 5 days in the case of Sentinel-2AB) and the relative speed of obtaining results allow for monitoring the condition of forests before and after the passage of a storm over large areas.

Another advantage of the proposed methodology is that the satellite images are readily available free of charge, and that they can be acquired for any area, making it possible to study changes in forest and non-forest areas at different latitudes. The only limitation for Sentinel-2 optical satellites is heavy cloud cover, as the emitted radiation does not penetrate clouds, rendering analysis of the study area impossible.

## Acknowledgements

The authors would like to express their thanks to Danuta Szumińska for her support and substantive commentary and Sebastian Czapiewski

for his assistance in conducting the study. They are also grateful to the Przymuszewo Forest Inspectorate for providing the data.

## References

- Chojnacka-Ożga L., Ożga W. 2018. Meteorological conditions of the occurrence of wind damage on August 11–12, 2017 in the forests of central–western Poland. *Sylwan* 162(3): 200–208. <https://doi.org/10.26202/sylwan.2017132>. [In Polish with English abstract]
- Ciesielski M., Bałazy R., Hycza T., Dmyterko E., Bruchwald A. 2016. Estimating the damage caused by the wind in the forest stands using satellite imagery and data from the State Forests Information System. *Sylwan* 160(5): 371–377. [In Polish with English abstract]
- Ciołkosz A., 2005. Teledetekcja satelitarna źródłem informacji o obiektach, zjawiskach i procesach zachodzących na Ziemi, *Nauka* 4, 51-70.

- Clarke M., Rendell H. 2007. Climate, extreme events and land degradation. [In:] M.V.K. Sivakumar, N. Ndiang'ui (Eds.) *Climate and Land Degradation*. Environmental Science and Engineering. Springer Berlin, Germany, 137-152, [https://doi.org/10.1007/978-3-540-72438-4\\_7](https://doi.org/10.1007/978-3-540-72438-4_7)
- Czapiewski S., Szumińska D. 2022. An Overview of Reote Sensing Data Applications in Peatland Research Based on Works from the Period 2010-2021. *Land* 11, 24. <https://doi.org/10.3390/land11010024>
- Dalponte M., Marzini S., Solano-Correa Y.T., Tonon G., Vescovo L., Gianelle D. 2020. Mapping forest windthrows using high spatial resolution multispectral satellite images. *International Journal of Applied Earth Observation and Geoinformation* 93, 102206. <https://doi.org/10.1016/j.jag.2020.102206>
- Diemientiew G. 2018. Extreme weather phenomenon in Poland in Times of climate change on the example of floods and strong winds. *Kultura Bezpieczeństwa, Nauka. Praktyka. Refleksje* 32, 79-100. <http://doi.org/10.5604/01.3001.0012.8094> [In Polish with English abstract].
- Dysarz R. 1998. Zarys geomorfologii i typy krajobrazu naturalnego w północnej części Borów Tucholskich. [In:] Banaszak J., Tobolski K. (Eds.), *Park Narodowy Bory Tucholskie. Stan poznania przyrody na tle kompleksu leśnego Bory Tucholskie*. Wydawnictwo Wyższej Szkoły Pedagogicznej, Bydgoszcz, 9-17 [In Polish]
- Escadafal R. 1989. Remote sensing of arid soil surface color with Landsat thematic mapper. *Advances in Space Resesearch* 9, 159-163.
- Forzieri G., Cescatti C., Silva F.B., Feyen L.E. 2017. Increasing risk over time of weather-related hazards to the European population: a data-driven prognostic study. *Lancet Planet Health* 1: e200-e208. [https://doi.org/10.1016/S2542-5196\(17\)30082-7](https://doi.org/10.1016/S2542-5196(17)30082-7)
- Frąckiewicz M., Palus H. 2011. KHM Clustering technique as a segmentation method for endoscopic colour images. *International Journal of Applied Mathematics Computer Science* 21(1), 203-209.
- Galon R. 1953. *Monografia doliny i sandru Brdy*. *Studia Societatis Scientiarum Toruniensis, Sectio C*, 1, 6, 1-54 [In Polish].
- Giannetti F., Pecchi M., Travaglini D., Francini S., D'Amico G., Vangi E., Coccozza C., Chirici G. 2021. Estimating VAIA Windstorm Damaged Forest Area in Italy Using Time Series Sentinel-2 Imagery and Continuous Change Detection Algorithms. *Forests* 12, 680. <https://doi.org/10.3390/f12060680>
- Haarsma R.J., Hazeleger W., Severijns C., de Vries H., Sterl A., Bintanja R., van Oldenborgh G. J., van den Brink H.W. 2013. More hurricanes to hit western Europe due to global warming. *Geophysical Research Letters* 40, 1783-1788. <https://doi.org/10.1002/grl.50360>
- Hejmanowska B., Wężyk P. 2020. *Dane satelitarne w administracji publicznej*. Wydawnictwo Polska Agencja Kosmiczna, Warszawa, 456, [In Polish].
- Hościło A., Lewandowska A. 2018. Zastosowanie danych z satelity Sentinel-2 do szacowania rozmiaru szkód spowodowanych w lasach huraganowym wiatrem w sierpniu 2017 roku. *Sylwan* 162(8), 619-627. <https://doi.org/10.26202/sylwan.2018055> [In Polish with English avstract].
- Instytut Meteorologii i Gospodarki Wodnej PIN, 2017, *Biuletyn Państwowej Służby Hydrologiczno-meteorologicznej*, sierpień, nr. 8 (184), ISSN 1730-6124 [In Polish].
- Jankowski M., Świtoniak M., Mendyk Ł. 2015. Stan pokrywy glebowej Tucholskiego Parku Krajobrazowego. [In:] Kunz M. (Ed.) *Monografia naukowa: Stan poznania środowiska przyrodniczego Tucholskiego Parku Krajobrazowego i Rezerwatu Biosfery Bory Tucholskie*. Polskie Wydawnictwa Reklamowe, Tuchola/Toruń, s. 31-43 [In Polish with English abstract]
- Kaczmarek J. 2018. *Klęska wiatrołomów na terenie Regionalnej Dyrekcji Lasów Państwowych w Toruniu*. Wydawnictwo Regionalna Dyrekcja Lasów Państwowych w Toruniu, p. 223, [In Polish].
- Karasiewicz T., Weckwerth P., Adamczyk A., Redzimska B. 2015. Budowa geologiczna i geomorfologia Tucholskiego Parku Krajobrazowego. [In:] Kunz M. (Ed.) *Monografia naukowa: Stan poznania środowiska przyrodniczego Tucholskiego Parku Krajobrazowego i Rezerwatu Biosfery Bory Tucholskie*. Polskie Wydawnictwa Reklamowe, Tuchola/Toruń, s. 15-30 [In Polish with English abstract]
- Kaufman L., Rousseeuw P.J. 1990. *Finding groups in data: An introduction to cluster analysis*. John Wiley and Sons Copyright, New York, USA, p. 342, <https://doi.org/10.1002/9780470316801>
- Kundzewicz Z., Matczak P. 2010, *Zagrożenia naturalnymi zdarzeniami ekstremalnymi*, *Nauka* 4, s. 77-86 [In Polish].
- Likas A., Vlassis N., Verbeek J. 2003. The global K-means clustering algorithm. *Pattern Recognition* 36, 451-461.
- Łabaj A. 2017. *Lotnicza inwentaryzacja uszkodzeń od wiatru w Nadleśnictwie Przymuszewo* – 02.10.2017 r.

- Okoniewska M., Szumińska D. 2020. Changes in Potential Evaporation in the Years 1952–2018 in North-Western Poland in Terms of the Impact of Climatic Changes on Hydrological and Hydrochemical Conditions, *Water* 12, 877. <https://doi.org/10.3390/w12030877>
- Olmo V., Tordoni E., Petruzzellis F., Bacaro G., Altobelli A. 2021. Use of Sentinel-2 Satellite Data for Windthrows Monitoring and Delimiting: The Case of “Vaia” Storm in Friuli Venezia Giulia Region (North-Eastern Italy). *Remote Sensing* 13, 1530. <https://doi.org/10.3390/rs13081530>
- Pettorelli N., Ryan S., Mueller M., Bunnefeld N., Jędrzejewska B., Lima M., Kausrud K. 2011. The Normalized difference Vegetation Index (NDVI): unforeseen successes in animal ecology. *Climate Research* 46(1), 15–27, <https://doi.org/10.1016/j.tree.2005.05.011>
- Piragnolo M., Pirotti F., Zanrosso C., Lingua E., Grigolato S. 2021. Responding to large-scale forest damage in an alpine environment with remote sensing, machine learning, and web-GIS. *Remote Sensing* 13, 1541. <https://doi.org/10.3390/rs13081541>
- Regionalna Dyrekcja lasów Państwowych w Toruniu, 2019. Plan Urządzenia Lasu Nadleśnictwa Przymuszewo na lata 2019–2028 [In Polish]
- Rouse J.W., Haas R.H., Schell J.A., Deering D.W. 1974. Monitoring Vegetation Systems in the Great Plains with ERTS. Third ERTS-1 Symposium NASA, NASA SP-351, Washington DC, USA, 309–317.
- Roy D.P., Wulder M.A., Loveland T.R., Woodcock C.E., Allen, R.G., Anderson M.C., Helder D., Irons J.R., Johnson D.M., Kennedy R., Scambos T.A., Schaaf C.B., Schott J.R., Sheng Y., Vermote E.F., Belward A.S., Bindschadler R., Cohen W.B., Gao F., Hipple J.D., Hostert P., Huntington J., Justice C.O., Kilic A., Kovalsky V., Lee Z.P., Lymburner L., Masek J.G., McCorkel J., Shuai Y., Trezza R., Vogelmann J., Wynne R.H., Zhu Z. 2014. Landsat 8: Science and product vision for terrestrial global change research. *Remote Sensing Environment* 145, 154–172. <http://dx.doi.org/10.1016/j.rse.2014.02.001>
- Šimić Milas A., Rupasinghe P., Balenović I., Grosevski P. 2015. Assessment of forest damage in Croatia using Landsat-8 OLI Images. *South-east European forestry* 6(2), 159–169. <http://dx.doi.org/10.15177/see-for.15-14>
- Starostwo Powiatowe w Chojnicach, Biuletyn Powiatu Chojnickiego, 2018. Klucz i brama, półrocze pod znakiem nawałnicy, Nr.5/2018, ISSN 2451-215X [In Polish]
- Sulik S., Kejna M. 2020. The origin and course of severe thunderstorm outbreaks in Poland on 10 and 11 August 2017, *Bulletin of Geography. Physical Geography Series* 18, 25–39. <https://doi.org/10.2478/bgeo-2020-0003>
- Szczepańska M. 2022a. Zmiany lesistości na terenie Borów Tucholskich po nawałnicy w 2017 roku i jej potencjalny wpływ na funkcjonowanie systemów rzecznych. Praca inżynierska, Instytut Geografii, Uniwersytet Kazimierza Wielkiego w Bydgoszczy [In Polish].
- Szczepańska M. 2022b. Wykorzystanie obrazów satelitarnych do analizy zmian wilgotności wybranych torowisk w Borach Tucholskich. Praca magisterska, Instytut Geografii, Uniwersytet Kazimierza Wielkiego w Bydgoszczy [In Polish].
- Tomaszewska M., Lewiński S., Woźniak E. 2011. Wykorzystanie zdjęć satelitarnych MODIS do badania stopnia pokrycia terenu roślinnością. *Teledetekcja środowiska* 46, 13–22 [In Polish].
- Trębski K. 2017. Największy kataklizm w historii Lasów Państwowych. <https://www.lasy.gov.pl/pl/informacje/aktualnosc/najwieksza-taka-kleska-w-historii-polskich-lasow>
- Urbański J. 2011. GIS w badaniach przyrodniczych. Wydawnictwo Uniwersytetu Gdańskiego, Gdańsk, p. 232, [In Polish].
- Wang W., Qu J.J., Hao X., Liu Y., Stanturf J.A. 2010. Post-Hurricane Forest Damage Assessment Using Satellite Remote Sensing. *Agricultural and Forest Meteorology* 150, 122–132. <https://doi.org/10.1016/j.agrformet.2009.09.009>
- Wesołowski T., Żmihorski M. 2018. Lasy po huraganach: uczyliśmy się na błędach. WWW.FORESTBIOLOGY.ORG Article 1, 1–7 [In Polish].
- Xie B., Ding J., Ge X., Li X., Han L., Wang Z. 2022. Estimation of Soil Organic Carbon Content in the Ebinur Lake Wetland, Xinjiang, China, Based on Multisource Remote Sensing Data and Ensemble Learning Algorithms. *Sensors* 22, 2685. <https://doi.org/10.3390/s22072685>
- Xue J., Su B. 2017. Significant remote sensing vegetation indices: A review of developments and application. *Jurnal of Sensors* 2017, Article ID: 1353691, <https://doi.org/10.1155/2017/1353691>
- Zarzecki M., Pasierbski A., 2009. Zastosowanie Gis i teledetekcji w badaniach szaty roślinnej, *Wiadomości Botaniczne* 53(3/4), 53–56 [In Polish].

Zhang X., Chen G., Cai L., Jiao H., Hua J., Luo X., Wei X., 2021. Impact Assessments of Typhoon Lekima on Forest Damages in Subtropical China Using Machine Learning Methods and Landsat 8 OLI Imagery. *Sustainability* 13, 4893. <https://doi.org/10.3390/su13094893>

#### **Internet sources**

ESA, 2019. Copernicus Open Access, <https://scihub.copernicus.eu/dhus/#/home> (Date of access: 21.10.2019).

IMGW, 2020. Dane pomiarowe obserwacyjne IMGW, <https://danepubliczne.imgw.pl> (Date of access: 16.03.2020).

Wetterzentrale.de, <https://www.wetterzentrale.de/> (Date of access: 10.04.2020).